DNA in CSF. The specificity and positive predictive value were very high, indicating that this method is highly reliable. HSV typing, which is important in the diagnosis of neonatal HSV infection [14, 15], was accurate with this method. However, the sensitivity of LAMP was 81%, whereas that of real-time PCR was 100%, indicating that the LAMP method is not as sensitive as real-time or nested PCR. This is probably due to the difference of sensitivity between the two methods. The real-time PCR can detect a minimum of five copies of either HSV-1 or HSV-2 DNA, while the HSV type-specific LAMP method detect a minimum of 500 copies of HSV-1 or 1000 copies of HSV-2 DNA per assay.

This study includes a considerable number of samples from neonates. We had shown previously that the viral loads in CSF were significantly higher in neonates than in older patients with HSV encephalitis [2, 10]. In neonatal HSV infection, HSV is frequently detected from the mucous membrane, even if there are no apparent vesicle lesions [23]. Swabs from throat, eye, or vesicles are widely used for the diagnosis of neonatal HSV infection. As shown in our previous experiments, the HSV type-specific LAMP is sensitive enough to detect viral DNA in swab samples [4]. Furthermore, direct amplification from swab samples is possible, which can omit DNA extraction step [4]. The type-specific HSV LAMP method may be potentially useful for the bedside diagnosis of neonatal HSV infection. Although further improvement in sensitivity is necessary for the wide spread use, this system might be applicable to diagnosis of HSV infection of the central nervous system.

Acknowledgements We thank the following people for their contributions to this study: Dr. Masahide Futamura (Aichi Prefectural Colony Hospital), Dr. Hisanori Sobajima (Nagoya City University School of Medicine), Dr. Masahiro Hayakawa (Nagoya University Hospital), Drs. Eiko Kato and Chizuko Suzuki (Nagoya First Red Cross Hospital), Dr. Makoto Ohshiro (Ogaki Municipal Hospital), Dr Youhei Tamura (the Jikei University School of Medicine), Dr. Toshiko Kubota (Kakegawa City General Hospital), Dr. Chie Nakamura (Higashi Municipal Hospital of Nagoya), Drs. Fumi Ishikawa and Toshiyuki Suzuki (Tsuchiura Kyodo General Hospital). This work was supported by a grant from the Ministry of Education, Culture, Sports, Science and Technology (16591022).

References

1. Aberle SW, Puchhammer-Stockl E (2002) Diagnosis of herpesvirus infections of the central nervous system. J Clin Virol 25(Suppl 1):S79–S85
2. Ando Y, Kimura H, Miwata H, Kudo T, Shibata M, Morishima T (1993) Quantitative analysis of herpes simplex virus DNA in cerebrospinal fluid of children with herpes simplex encephalitis. J Med Virol 41:170–173
3. Aurelius E, Johansson B, Skoldenberg B, Staland A, Forsgren M (1991) Rapid diagnosis of herpes simplex encephalitis by nested polymerase chain reaction assay of cerebrospinal fluid. Lancet 337:189–192
4. Enomoto Y, Yoshikawa T, Ihira M, Akimoto S, Miyake F, Usui C, Suga S, Suzuki K, Kawana T, Nishiyama Y, Asano Y (2005) Rapid diagnosis of herpes simplex virus infection by loop-mediated isothermal amplification method. J Clin Microbiol 43:951–955
5. Enosawa M, Kageyama S, Sawai K, Watanabe K, Notomi T, Onoe S, Mori Y, Yokomizo Y (2003) Use of loop-mediated isothermal amplification of the IS900 sequence for rapid detection of cultured Mycobacterium avium subsp. paratuberculosis. J Clin Microbiol 41:4359–4365
6. Hong TC, Mai QL, Cuong DV, Parida M, Minekawa H, Notomi T, Hasebe F, Morita K (2004) Development and evaluation of a novel loop-mediated isothermal amplification method for rapid detection of severe acute respiratory syndrome coronavirus. J Clin Microbiol 42:1956–1961
7. Ihira M, Yoshikawa T, Enomoto Y, Akimoto S, Ohashi M, Suga S, Nishimura N, Ozaki T, Nishiyama Y, Notomi T, Ohta Y, Asano Y (2004) Rapid diagnosis of human herpesvirus 6 infection by a novel DNA amplification method, loop-mediated isothermal amplification. J Clin Microbiol 42:140–145
8. Ito Y, Kimura H, Yabuta Y, Ando Y, Murakami T, Shiomi M, Morishima T (2000) Exacerbation of herpes simplex encephalitis after successful treatment with acyclovir. Clin Infect Dis 30:185–187
9. Iwamoto T, Sonobe T, Hayashi K (2003) Loop-mediated isothermal amplification for direct detection of Mycobacterium tuberculosis complex, M. avium, and M. intracellulare in sputum samples. J Clin Microbiol 41:2616–2622
10. Kawada J, Kimura H, Ito Y, Hoshino Y, Tanaka-Kitajima N, Ando Y, Futamura M, Morishima T (2004) Comparison of real-time and nested PCR assays for detection of herpes simplex virus DNA. Microbiol Immunol 48:411–415
11. Kessler HH, Muhlbauer G, Rinner B, Stelzl E, Berger A, Dorr HW, Santner B, Marth E, Rabenau H (2000) Detection of Herpes simplex virus DNA by real-time PCR. J Clin Microbiol 38:2638–2642
12. Kimberlin DW, Lakeman FD, Arvin AM, Prober CG, Corey L, Powell DA, Burchett SK, Jacobs RF, Starr SE, Whitley RJ (1996) Application of the polymerase chain reaction to the diagnosis and management of neonatal herpes simplex virus disease. National Institute of Allergy and Infectious Diseases Collaborative Antiviral Study Group. J Infect Dis 174:1162–1167
13. Kimura H, Aso K, Kuzushima K, Hanada N, Shibata M, Morishima T (1992) Relapse of herpes simplex encephalitis in children. Pediatrics 89:891–894
14. Kimura H, Futamura M, Ito Y, Ando Y, Hara S, Sobajima H, Nishiyama Y, Morishima T (2003) Relapse of neonatal herpes simplex virus infection. Arch Dis Child Fetal Neonatal Ed 88:F483–F486
15. Kimura H, Ito Y, Futamura M, Ando Y, Yabuta Y, Hoshino Y, Nishiyama Y, Morishima T (2002) Quantitation of viral load in neonatal herpes simplex virus infection and comparison between type 1 and type 2. J Med Virol 67:349–353
16. Kimura H, Morita M, Yabuta Y, Kuzushima K, Kato K, Kojima S, Matsuyama T, Morishima T (1999) Quantitative analysis of Epstein-Barr virus load by using a real-time PCR assay. J Clin Microbiol 37:132–136
17. Klapper PE, Cleator GM (1998) European guidelines for diagnosis and management of patients with suspected herpes simplex encephalitis. Clin Microbiol Infect 4:178–180
18. Lakeman FD, Whitley RJ (1995) Diagnosis of herpes simplex encephalitis: application of polymerase chain reaction to cerebrospinal fluid from brain-biopsied patients and correlation with disease. National Institute of Allergy and Infectious Diseases Collaborative Antiviral Study Group. J Infect Dis 171:857–863
19. Mori Y, Kitao M, Tomita N, Notomi T (2004) Real-time turbidimetry of LAMP reaction for quantifying template DNA. J Biochem Biophys Methods 59:145–157
20. Nagamine K, Hase T, Notomi T (2002) Accelerated reaction by loop-mediated isothermal amplification using loop primers. Mol Cell Probes 16:223–229

21. Notomi T, Okayama H, Masubuchi H, Yonekawa T, Watanabe K, Amino N, Hase T (2000) Loop-mediated isothermal amplification of DNA. Nucleic Acids Res 28:E63
22. Parida M, Posadas G, Inoue S, Hasebe F, Morita K (2004) Real-time reverse transcription loop-mediated isothermal amplification for rapid detection of West Nile virus. J Clin Microbiol 42:257–263
23. Whitley RJ (2001) Herpes simplex virus. In: Knipe DM, Howly PM (eds) Virology, vol. 2. Lippincott Williams & Wilkins, Philadelphia, pp 2461–2510
24. Yoshikawa T, Ihira M, Akimoto S, Usui C, Miyake F, Suga S, Enomoto Y, Suzuki R, Nishiyama Y, Asano Y (2004) Detection of human herpesvirus 7 DNA by loop-mediated isothermal amplification. J Clin Microbiol 42:1348–1352

Pediatr Allergy Immunol 2005: 16: 357–360

PEDIATRIC ALLERGY AND IMMUNOLOGY
DOI: 10.1111/j.1399-3038.2005.00279.x

Case Report

A common variable immunodeficient patient who developed acute disseminated encephalomyelitis followed by the Lennox-Gastaut syndrome

Kondo M, Fukao T, Teramoto T, Kaneko H, Takahashi Y, Okamoto H, Kondo N. A common variable immunodeficient patient who developed acute disseminated encephalomyelitis followed by the Lennox-Gastaut syndrome.
Pediatr Allergy Immunol 2005: 16: 357–360. © 2005 Blackwell Munksgaard

Common variable immunodeficiency (CVID) is a primary disorder characterized by impaired antibody production. CVID patients may develop recurrent infections, autoimmune disorders, and malignant lymphomas, but to our knowledge, there is no report on CVID patients who develop acute disseminated encephalomyelitis (ADEM) or the Lennox-Gastaut syndrome. We describe a 1-yr-old female CVID patient with ADEM who evolutionally manifested the Lennox-Gastaut syndrome. She was admitted with convulsions and T2-weighted magnetic resonance imaging (MRI) revealed high-intensity areas in the right temporal lobe and the left fronto-parietal region but she became conscious soon. Her serum findings showed severe hypogammaglobulinemia and a follow up MRI revealed that these areas had diminished. Consequently, she was diagnosed as having CVID with ADEM. After 5 months, she fell to having tonic and absence seizures and we diagnosed her as having the Lennox-Gastaut syndrome from electroencephalograms (EEG) and the seizure pattern. She is now 7 yr old and her tonic seizures are controlled with valproic acid, clobazam, and immunoglobulin replacement therapy which is administrated every 2 wk. It is well known that the immune and neurologic systems have a close relationship. We suspect that a genetic defect in the immune system of our patient might also be associated with the neurologic disorders of ADEM and the Lennox-Gastaut syndrome.

Masashi Kondo[1], Toshiyuki Fukao[1], Takahide Teramoto[1], Hideo Kaneko[1], Yukitoshi Takahashi[1], Hiroyuki Okamoto[2] and Naomi Kondo[1]

[1]Department of Pediatrics, Graduate School of Medicine, Gifu University, Gifu, [2]Department of Pediatrics, Kizawa Memorial Hospital, Minokamo, Gifu, Japan

Key words: common variable immunodeficiency; hypogammaglobulinemia; acute disseminated encephalomyelitis; magnetic resonance imaging; Lennox-Gastaut syndrome; experimental allergic encephalomyelitis; autoimmune disease; CD4; CD8

Masashi Kondo, Department of Pediatrics, Graduate School of Medicine, Gifu University, Yanagido 1-1, Gifu 501-1194, Japan
Tel.: +81-58-230-6386
Fax: +81-58-230-6387
E-mail: g2104012@guedu.cc.gifu-u.ac.jp

Accepted 21 February 2005

Common variable immunodeficiency syndrome (CVID) is the most common symptomatic primary antibody-deficient syndrome, characterized by hypogammaglobulinemia, and most patients have recurrent pyogenic infections predominantly in the upper and lower respiratory and gastrointestinal tracts (1). CVID patients are prone to malignancies such as gastric carcinoma and lymphoma, and to autoimmune and granulomatous diseases (1). Acute disseminated encephalomyelitis (ADEM) is an inflammatory demyelinating disorder related to autoimmunity (2), the typical clinical features of which are characterized by the acute onset of multifocal neurologic signs and may include impaired consciousness, convulsions, psychotic symptoms, or behavioral change (3). This disorder is usually associated with preceding infections or vaccinations (4). Only nine patients with CVID-associated encephalomyelitis have been reported in the literature (1, 5, 6). Virus infections such as an enterovirus have been identified as the cause of encephalomyelitis in some cases, but an autoimmune central nervous system disease has also been considered in other cases (5).

To our knowledge there is no report on CVID patients who develop ADEM. In this report, we present a CVID patient with ADEM, who evolutionally manifested the Lennox-Gastaut syndrome.

Case report

A 1-yr-old female was hospitalized in May 1998 with a fever, impaired consciousness, and right hemi-convulsions. Two weeks before admission, she suffered from otitis media with effusion and had taken antibiotics for 2 wk. There was no family history of neurologic disorders or immunodeficiency, and her developmental milestones were within the normal range until her hospitalization. On neurologic examination in the post-convulsive state, upward nystagmus and intention tremors were observed. Hematologic examination showed mild anemia [hemoglobin (Hb) 9.7 g/dl] and lymphocytosis [white blood cell (WBC) counts 11,000/mm^3; lymphocytes 70.8%] and biochemical analyses were not significant except for a mild elevation of the C-reactive protein (CRP; 0.68 mg/dl; control range: 0.00–0.50). The cerebrospinal fluid (CSF) was clear, with normal pressure, 10 leukocytes/mm^3 (mononuclear cells 8/mm^3; neutrophils 2/mm^3), glucose 88 mg/dl, and protein 24 mg/dl. Bacterial culture was negative. An electroencephalogram (EEG) showed diffuse high-voltage slow waves at the left hemisphere and spindles mainly at the right frontal region. Brain magnetic resonance imaging (MRI) depicted areas of increased signal intensity in subcortical white matter in the right temporal lobe and the left fronto-parietal region on T2-weighted images (Fig. 1). This patient became conscious soon and developed no further symptoms. A follow up EEG showed the disappearance of diffuse high-voltage slow waves on the left hemisphere. She did not receive methylprednisolone pulse therapy or high-dose immunoglobulin therapy. She was prescribed carbamazepine (CBZ), 50 mg/day, and discharged on the 11 hospital day. One month later, a follow up MRI revealed that areas of high intensity had diminished on the T2-weighted images. Retrospectively, she was diagnosed as having ADEM.

She was again admitted with a cough and a low-grade fever in July 1998 to this hospital. Hematologic and serum laboratory tests showed a WBC count of 3800/mm^3 with 25.0% neutrophils, 47.7% lymphocytes, 22.6% monocytes, and 3.6% eosinophils; red blood cell (RBC) count 515×10^4/mm^3; Hb 8.7/dl; Ht 25.4%; platelet count 170×10^3/mm^3; aspartate aminotransferase (AST) 17 IU/l; alanine aminotransferase (ALT) 6 IU/l; CRP 6.81 mg/dl; immunoglobulin G (IgG) 14 mg/dl (control range: 516–990); IgA 2 mg/dl (21–140); IgM 22 mg/dl (42–159); IgE, 1 IU/ml (5–30). On examination, she had mild wheezing and her cervical lymph nodes were palpable normally. She was diagnosed as having bronchitis with hypogammaglobulinemia. Retrospective examination of frozen sera from the first admission also revealed hypogammaglobulinemia (IgG 79 mg/dl; IgA 5 mg/dl; IgM 16 mg/dl). Lymphocyte surface marker data were as follows: CD3+, 78% (62–69); CD4+, 72.9% (30–40); CD8+, 5.9% (25–32); CD19+, 11% (21–28); surface IgM+, 8% (3–12); surface IgG+, 0% (1–3); surface IgA+, 0% (1–3); surface IgD+, 10% (1–10; κ+, 5% (3–8); λ+, 4% (1–5). Adenosine deaminase activity was 33.6 U/l (9–19). Lymphocyte proliferation was normal by stimulation with phytohemagglutinin (PHA; mitotic index: 261) and concanavalin A (mitotic index: 235).

She was referred to Gifu University Hospital for further immunologic examination. We analyzed the ability of IgM and IgG secretion in peripheral blood mononuclear cells (PBMCs) according to the method reported by Bryant et al. (7). However, the PBMCs derived from the patient did not secrete detectable levels of IgM and IgG (data not shown), so this patient was revealed to belong to group A CVID. Thereafter, she has received immunoglobulin replacement therapy once a month from September 1998 and has never developed a severe bacterial infection thus far.

In October 1998, she fell into a 'drowsy' state and started to have tonic seizures, upon which she was again admitted to our hospital. A brain MRI revealed no high-intensity areas on T2-weighted images and EEG recordings demonstrated a diffuse rapid rhythm in the sleeping state. She had myoclonic, tonic and absence seizures and was diagnosed as having the Lennox-Gastaut syndrome. Valproic acid (VPA) was added to CBZ, but the seizures occurred frequently and developmental delay became more evident. Several combinations of antiepileptic drugs (zonisamide, phenytoin), methylprednisolone pulse therapy, and high-dose immunoglobulin therapy (400 mg/kg/day) could not control her seizures. From July 2000, a new combination of immunoglobulin replacement therapy (every 2 wk), VPA and clobazam, reduced the seizure frequency. She is now 7 yr old and her tonic seizures are under control, but her psychomotor developmental age is about 3 yr old.

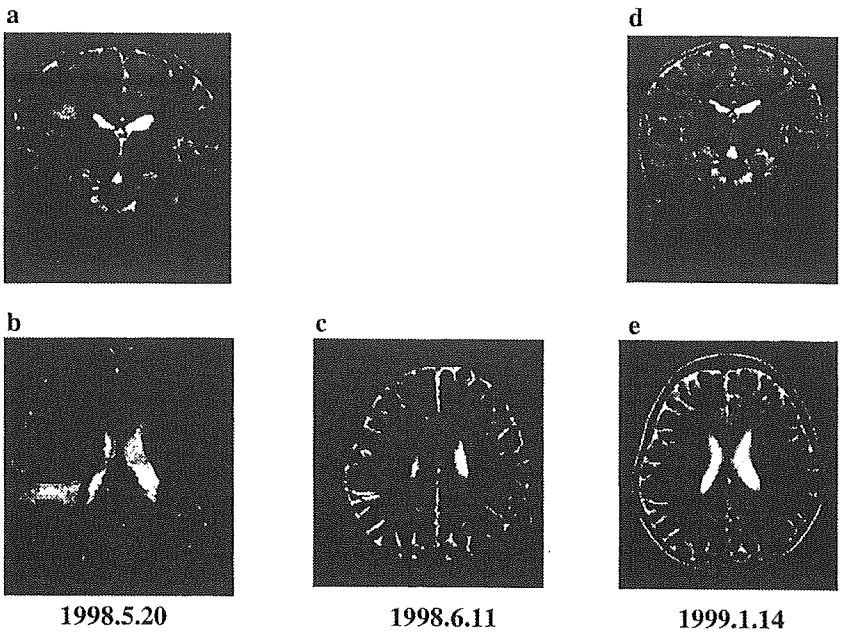

Fig. 1. (a and b) Non-contrast axial and coronal T2-weighted magnetic resonance imaging (MRI), obtained after first convulsions, demonstrates high intensity in subcortical white matter in the right temporal lobe and left fronto-parietal region. (c) Axial T2-weighted MRI at 4 wk after admission; high-intensity areas had almost disappeared. (d and e) Axial and coronal T2-weighted MRI at 6 months after first admission, when diagnosed as having the Lennox-Gastaut syndrome; abnormal areas had improved.

Discussion

This CVID patient developed ADEM followed by the Lennox-Gastaut syndrome. CVID is the most common symptomatic primary antibody-deficient syndrome and has a heterogeneous etiology (8). In most cases, the gene defects responsible for CVID are unknown. The characteristic immunologic features in this patient are (i) decreased serum IgM, IgG, and IgA, (ii) normal number of surface IgM- and IgD-positive B cells, (iii) no IgG and IgM secretion from B cells stimulated with CD40 and interleukin (IL)-4, (iv) decreased number of CD8+ lymphocytes, and (v) normal natural killer (NK) cell activity. We have been investigating the defects in this patient at the molecular level but have failed to identify the cause thus far.

It is known that approximately 20% of patients with CVID develop one or more autoimmune diseases such as autoimmune hemolytic anemia, autoimmune thrombocytopenia, rheumatoid arthritis, and pernicious anemia (1), indicating that CVID is a disease of abnormal immunity regulation as well as an immunodeficiency. This patient developed ADEM, which is an inflammatory demyelinating disorder related to autoimmunity (4), so it is possible that CVID patients develop ADEM. However, to our knowledge, there is no report on ADEM in CVID patients. ADEM is believed to be the clinical counterpart of experimental allergic encephalomyelitis (EAE) (9). CD4+ myelin-specific T cells induced EAE (10). The role of CD8+ T lymphocytes has been described as having both effector and suppressor functions in the pathogenesis of EAE (11). This CVID patient has the peculiar feature of an increased ratio of CD4/CD8 and a reduced number of CD8+ T lymphocytes. This unbalance of the T-cell subpopulation may be associated with the development of ADEM in this patient.

The diagnosis of ADEM in our patient depended on MRI (2). Although the clinical symptoms disappeared without steroid or immunoglobulin therapy, asymmetrical and multiple T2 high lesions in subcortical white matter were noted when she developed the first convulsive state and then subsequently disappeared 4 wk later. This finding highly supports the diagnosis of ADEM.

The Lennox-Gastaut syndrome is characterized by tonic seizures associated with myoclonic seizures, atypical absence seizures, rapid rhythm in the sleeping state, and cognitive impairment (12). The etiologies of this syndrome have been divided into symptomatic and cryptogenic types, the former being attributed to brain disorders such as meningitis, encephalitis, head injury, and cerebrovascular diseases (13). ADEM might be etiologically related to the Lennox-Gastaut syndrome in our patient, as ADEM sometimes involves not only white matter but also gray matter (2). However, to our knowledge, the Lennox-Gastaut syndrome has not been reported as a sequela of ADEM.

The CVID is a syndrome caused by heterogeneous genetic defects. It is well known that the immune and neurologic systems have a close relationship. We suppose that the genetic defect in our patient might also be associated with the neurologic disorders of ADEM and the Lennox-Gastaut syndrome. It is of interest to identify the gene defect in this patient.

References

1. Cunningham-Rundles C, Bodian C. Common variable immunodeficiency: clinical and immunological features of 248 patients. Clin Immunol 1999: 92: 34–48.
2. Kesselring J, Miller DH, Robb SA, et al. Acute disseminated encephalomyelitis. MRI findings and the distinction from multiple sclerosis. Brain 1990: 113: 291–302.
3. Lee WT, Wang PJ, Liu HM, et al. Acute disseminated encephalomyelitis in children: clinical, neuroimaging and neurophysiologic studies. Acta Pediatr Sin 1996: 37: 197–203.
4. Tenembaum S, Chamoles N, Fejerman N. Acute disseminated encephalomyelitis: a long-term follow-up study of 84 pediatric patients. Neurology 2002: 59: 1224–31.
5. Rudge P, Webster AD, Revesz T, et al. Encephalomyelitis in primary hypogammaglobulinaemia. Brain 1996: 119: 1–15.
6. Happe S, Husstedt IW. Successful treatment of acute encephalomyelitis associated with common variable immunodeficiency syndrome (CVID): case report and review of the literature. J Neurol 2000: 247: 562–5.
7. Bryant A, Calver NC, Toubi E, Webster AD, Farrant J. Classification of patients with common variable immunodeficiency by B cell secretion of IgM and IgG in response to anti-IgM and interleukin-2. Clin Immunol Immunopathol 1990: 56: 239–48.
8. Spickett GP, Farrant J, North ME, Zhang JG, Morgan L, Webster AD. Common variable immunodeficiency: how many diseases? Immunol Today 1997: 18: 325–8.
9. Gold R, Hartung HP, Toyka KV. Animal models for autoimmune demyelinating disorders of the nervous system. Mol Med Today 2000: 6: 88–91.
10. Lafaille JJ, Nagashima K, Katsuki M, Tonegawa S. High incidence of spontaneous autoimmune encephalomyelitis in immunodeficient anti-myelin basic protein T cell receptor transgenic mice. Cell 1994: 78: 399–408.
11. Koh DR, Fung-Leung WP, Ho A, Gray D, Acha-Orbea H, Mak TW. Less mortality but more relapses in experimental allergic encephalomyelitis in CD8−/− mice. Science 1992: 256: 1210–3.
12. Gastaut H, Roger J, Soulayrol R, et al. Childhood epileptic encephalopathy with diffuse slow spike-waves (otherwise known as 'peit mal variant') or Lennox syndrome. Epilepsia 1966: 7: 139–79.
13. Riikonen R. Long-term outcome of West syndrome: a study of adults with a history of infantile spasms. Epilepsia 1996: 37: 367–72.

Effect of montelukast on nuclear factor κB activation and proinflammatory molecules

Shinji Maeba, MD; Takashi Ichiyama, MD; Yoshiko Ueno, PhD; Haruyuki Makata, MD; Tomoyo Matsubara, MD; and Susumu Furukawa, MD

Background: Montelukast is known as a cysteinyl leukotriene 1 receptor antagonist. However, the action of montelukast in terms of nuclear factor κB (NF-κB) activation and the production of proinflammatory molecules is unknown.

Objective: To demonstrate the potential anti-inflammatory effect of montelukast.

Methods: We examined whether montelukast inhibits the activation of NF-κB, a transcription factor that regulates the expression of proinflammatory molecules. The inhibitory effects of montelukast on tumor necrosis factor α (TNF-α)–induced NF-κB activation on THP-1 cells, a human monocytic leukemia cell line, were evaluated by flow cytometry, and those on lipopolysaccharide-induced interleukin 1β (IL-1β), IL-6, TNF-α, and monocyte chemoattractant protein 1 (MCP-1) production in peripheral blood mononuclear cells were evaluated by enzyme-linked immunosorbent assay.

Results: Flow cytometry demonstrated that montelukast inhibited NF-κB activation in THP-1 cells in a dose-related manner. Furthermore, 10^{-5}M montelukast significantly inhibited lipopolysaccharide-induced IL-6, TNF-α, and MCP-1 production in the peripheral blood mononuclear cells of controls and patients with asthma. Lipopolysaccharide-induced IL-1β production was not inhibited by montelukast.

Conclusions: These findings suggest that high doses of montelukast modulate the production of IL-6, TNF-α, and MCP-1 through the inhibition of NF-κB activation. However, the anti-inflammatory effect of montelukast at therapeutic doses in patients with asthma needs to be further investigated.

Ann Allergy Asthma Immunol. 2005;94:670–674.

INTRODUCTION

Montelukast antagonizes the cysteinyl leukotriene 1 (CysLT1) receptor and inhibits the contraction of the tracheal muscle induced by leukotriene D_4.[1,2] Furthermore, montelukast has an anti-inflammatory effect on asthma.[3,4] Nuclear factor κB (NF-κB) is a transcription factor for genes that encode proinflammatory molecules such as interleukin 1 (IL-1), IL-2, IL-6, IL-8, IL-12, tumor necrosis factor α (TNF-α), and monocyte chemoattractant protein 1 (MCP-1).[5–9] The prototype of NF-κB is a heterodimer that consists of p50 and p65 bound by members of the IκB family, including IκBα, in the cytoplasm.[10,11] Phosphorylation of IκB by bacteria, viruses, and cytokines rapidly leads to IκB degradation and translocation of NF-κB to the nucleus.[12,13] Activation of NF-κB results in the binding of specific promoter elements and the expression of messenger RNAs for proinflammatory molecule genes.[5–9]

Bacterial and viral infections often induce bronchial asthma attacks, especially in children. It is important to modulate infectious inflammation in the treatment of patients with bronchial asthma. Monocytes and macrophages play an essential role in the infectious inflammatory response and in the allergic inflammation. Therefore, we tested the hypothesis that montelukast modulates inflammation by inhibiting NF-κB activation in human monocytic THP-1 cells and peripheral blood mononuclear cells (PBMCs).

Department of Pediatrics, Yamaguchi University School of Medicine, Yamaguchi, Japan.

Received for publication July 5, 2004.
Accepted for publication in revised form January 14, 2005.

MATERIALS AND METHODS

Cell Culture and Stimulation Conditions

THP-1 cells, a human monocytic leukemia cell line, obtained from the American Type Culture Collection, were maintained at 37°C under humidified 5% carbon dioxide as a stationary culture. The cells were grown in RPMI 1640 medium containing 10% fetal bovine serum, 100 U/mL of penicillin, and 100 μg/mL of streptomycin. The PBMCs were obtained from heparinized blood samples from 8 healthy, medication-free volunteers and 8 patients with asthma, with informed consent, using the Histopaque 1077 (Sigma-Aldrich Corp, St Louis, MO) gradient centrifugation, and then resuspended in RPMI 1640 medium containing 10% fetal bovine serum, 100 U/mL of penicillin, and 100 μg/mL of streptomycin. Cells were exposed to 2 ng/mL of TNF-α (R&D Systems Inc, Minneapolis, MN) for 30 minutes or 1 μg/mL of lipopolysaccharide (from *Escherichia Coli*, 0111:B4; Sigma-Aldrich Corp) for 2 hours, with or without 30 minutes of pretreatment with 10^{-7}, 10^{-6}, or 10^{-5}M montelukast (Merck & Co, Whitehouse Station, NJ).

CysLT1 Receptors

THP-1 cells were first labeled with a rabbit anti–CysLT1 receptor polyclonal antibody (Cayman, Ann Arbor, MI) and then with a fluorescein isothiocyanate–conjugated goat anti–rabbit IgG monoclonal antibody (Sigma-Aldrich Corp). Im-

ages were acquired, processed, and quantified using a microscope (Olympus BX50; Olympus, Tokyo, Japan), a CCD camera (Micromac; Princeton Instruments, San Diego, CA), and an imaging system (MetaMorph; Universal Imaging Corp, West Chester, PA).

Flow Cytometric Analysis

Flow cytometric analysis was performed according to the previously published procedure.[14,15] The cells were permeabilized with 4% paraformaldehyde in phosphate-buffered saline, pH 7.2, containing 0.1% saponin and 10-mmol/L HEPES. The cells were then labeled with a mouse anti–NF-κB (nuclear-localized signal) antibody (IgG3; Chemicon International Inc, Temecula, CA). The mouse anti–NF-κB (nuclear-localized signal) antibody recognizes an epitope overlapping the nuclear location signal of NF-κB–p65 and therefore selectively recognizes the activated form of NF-κB. The cells were then labeled with a fluorescein isothiocyanate–conjugated rat anti–mouse IgG3 monoclonal antibody (PharMingen, San Diego, CA). After washing, the cells were fixed with 1% paraformaldehyde in phosphate-buffered saline and then stored at 4°C until flow cytometric analysis. Single-color immunofluorescence analysis of approximately 5,000 cells was performed using a FACScan flow cytometer equipped with CellQuest software (BD Biosciences, San Jose, CA).

Determination of IL-1β, IL-6, TNF-α, and MCP-1 Concentrations

The PBMCs were seeded into 6-well tissue culture dishes at a density of 1×10^6 cells per well and then exposed to 1 μg/mL of lipopolysaccharide, with or without pretreatment with montelukast for 30 minutes. The culture fluid was collected 2 hours after lipopolysaccharide addition. The concentrations of IL-1β, IL-6, TNF-α, and MCP-1 in the samples were determined using a sandwich-type enzyme-linked immunosorbent assay (ELISA) kit (R&D Systems Inc). The detection limits for IL-1β, IL-6, TNF-α, and MCP-1 were 1.0, 3.1, 1.6, and 5.0 pg/mL, respectively.

Statistical Analysis

Statistical analysis was performed using the Wilcoxon matched paired test. $P < .05$ was considered statistically significant.

RESULTS

An immunofluorescence microscopic image demonstrated that THP-1 cells had CysLT1 receptors on their membranes (Fig 1). Flow cytometric analysis demonstrated that montelukast inhibited TNF-α–induced NF-κB activation in THP-1 cells in a dose-related manner (Fig 2). Nuclear factor κB activation was inhibited by 10^{-5}M and 10^{-6}M montelukast by approximately 27% ($P = .009$) and 8% ($P = .02$), respectively (Fig 3).

The ELISA demonstrated that 10^{-5}M montelukast inhibited lipopolysaccharide-induced IL-6, TNF-α, and MCP-1 production in culture fluid of the PBMCs of controls by approximately 53% ($P < .001$), 13% ($P = .005$), and 8% ($P = .005$), respectively (Fig 4). The mean ± SD IL-1β concentration in culture fluid of the PBMCs of controls exposed only to lipopolysaccharide was 67.6 ± 32.5 pg/10^6 cells. The production of IL-1β was not significantly inhibited by 10^{-7}M, 10^{-6}M, or 10^{-5}M montelukast (mean ± SD: 60.8 ± 19.6 pg/10^6 cells, $P = .499$; 70.1 ± 36.6 pg/10^6 cells; $P = .39$; and 70.0 ± 21.2 pg/10^6 cells, $P = .499$, respectively). The ELISA demonstrated that montelukast inhibited lipopolysaccharide-induced IL-6, TNF-α, and MCP-1 production in culture fluid of the PBMCs of patients with asthma by approximately 49% ($P < .001$), 16% ($P = .004$), and 12% ($P = .005$), respectively (Fig 5). The lipopolysaccharide-induced IL-1β production in culture fluid of the PBMCs of patients with asthma was not significantly inhibited by montelukast. The inhibitory effects of montelukast on lipopolysaccharide-induced IL-6, TNF-α, and MCP-1 production in culture fluid of the PBMCs of patients with asthma were similar to those of controls.

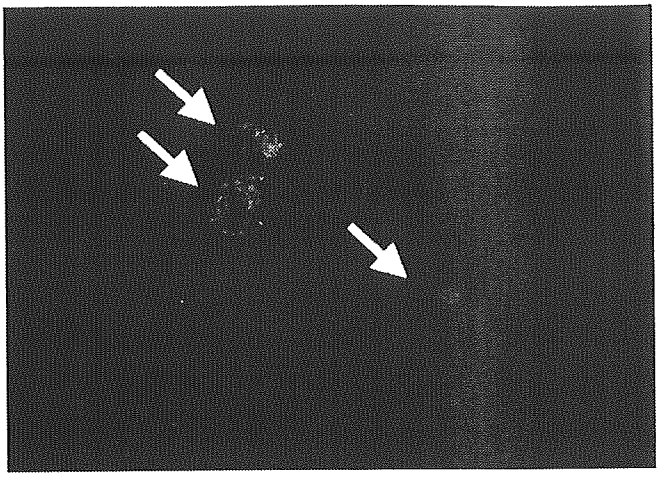

Figure 1. Immunofluorescent microscopic image showing THP-1 cells labeled with anti–cysteinyl leukotriene 1 receptor antibodies and fluorescein isothiocyanate–conjugated secondary antibodies (arrows)

DISCUSSION

Recently, Ichiyama et al[16] demonstrated that pranlukast, a CysLT1 receptor antagonist, inhibited NF-κB activation in human monocytic U-937 cells, which had CysLT1 receptors on the cell membranes, and in human T-cell Jurkat cells, which did not have CysLT1 receptors on the cell membranes, and modulated IL-6 production stimulated by lipopolysaccharide in PBMCs. They also demonstrated that pranlukast inhibited NF-κB activation in U-937 cells more than in Jurkat cells, whereas the CysLT1 receptor would not be involved in the inhibition of NF-κB activation. Pranlukast is a leukotriene C_4, D_4, and E_4 receptor antagonist, and montelukast is a potent and selective leukotriene D_4 receptor antagonist.[1,17] In the present study, we revealed that montelukast also inhibited NF-κB activation in human monocytic THP-1 cells. Experi-

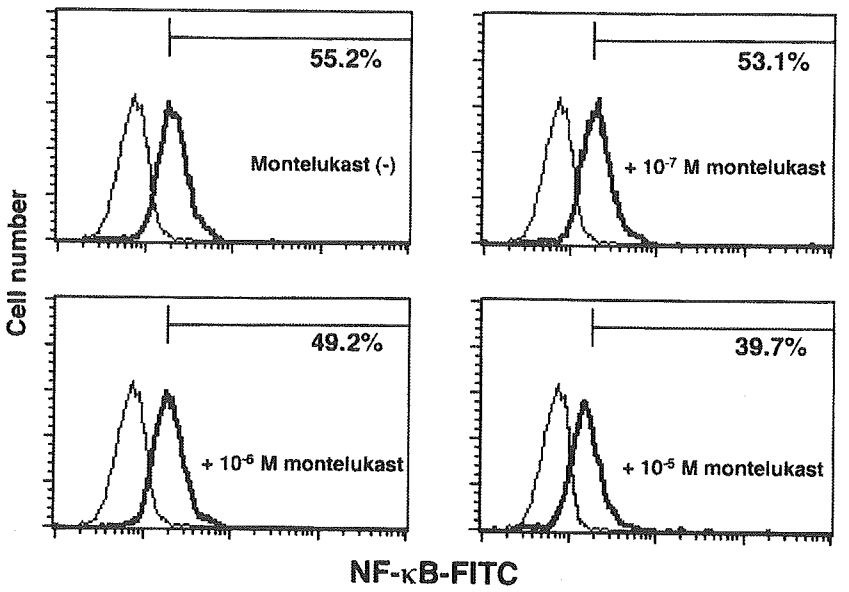

Figure 2. Representative flow cytometric analysis demonstrated that pretreatment with montelukast inhibited nuclear factor κB (NF-κB) activation induced by tumor necrosis factor α in THP-1 cells. Activated NF-κB is shown by a thick line, and the background isotype antibody binding is shown by a thin line for each sample. A line of 0.9% to 1.0% positive cells in the background was determined as a cutoff line. An area of the thick line on the right of the cutoff line is the percentage of positive cells. FITC indicates fluorescein isothiocyanate.

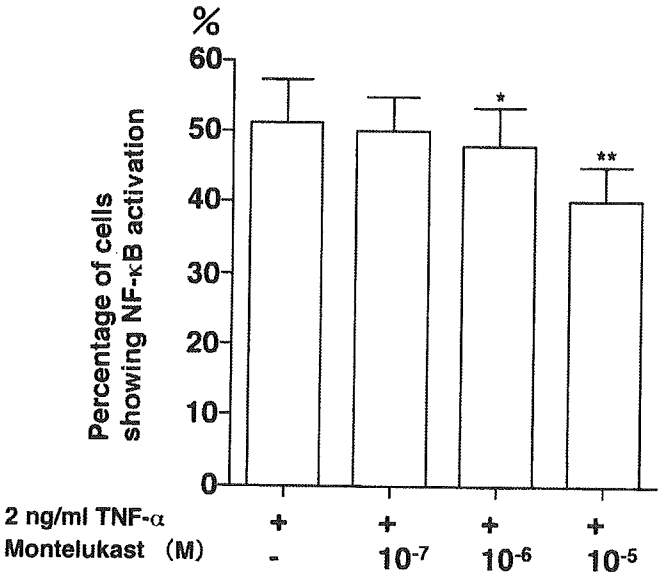

Figure 3. Inhibitory effect of montelukast on nuclear factor κB (NF-κB) activation, as measured by flow cytometric analysis, in THP-1 cells stimulated with tumor necrosis factor α (TNF-α) for 30 minutes, with pretreatment with montelukast for 30 minutes. Data (n = 8) are presented as mean +1 SD. Double asterisk indicates $P < .01$; asterisk, $P < .05$ compared with cells treated with TNF-α only.

ments using normal peripheral blood CD14$^+$ monocytes instead of THP-1 cells are preferable. However, the numbers of normal peripheral blood CD14$^+$ monocytes obtained from 1 volunteer were too few to perform the experiments. Therefore, we did the experiments using THP-1 cells.

We demonstrated that montelukast inhibited the lipopolysaccharide-induced production of not only IL-6 but also TNF-α and MCP-1 in the PBMCs of controls and patients with asthma. There was no difference of the inhibitory effects of montelukast on the PBMCs of controls and patients with asthma. Montelukast did not inhibit lipopolysaccharide-induced IL-1β production in the PBMCs of controls or patients with asthmas. The detail of the mechanism as to why montelukast did not inhibit lipopolysaccharide-induced IL-1β production is unclear. The production of each proinflammatory molecule is controlled by many factors, such as the intracellular stimulation of transcription factors or the extracellular stimulation of proinflammatory molecules. Therefore, it is likely that the proinflammatory molecules whose transcription is controlled by NF-κB did not show similar movements in just 1 experiment.

The underlying mechanism of the inhibitory effect on NF-κB activation by montelukast is unclear. Taking a previous study into consideration,[16] antagonism of CysLT1 receptors may be partially related to the inhibition of NF-κB activation, and it is likely that CysLT1 receptor antagonists have another mechanism that inhibits NF-κB activation. Antagonists of the CysLT1 receptor compose a new class of drugs, which is being actively studied, and further research will expand our knowledge of their anti-inflammatory potential.

Bacterial and viral infections are important triggers in many children with bronchial asthma.[18–20] Monocytes and

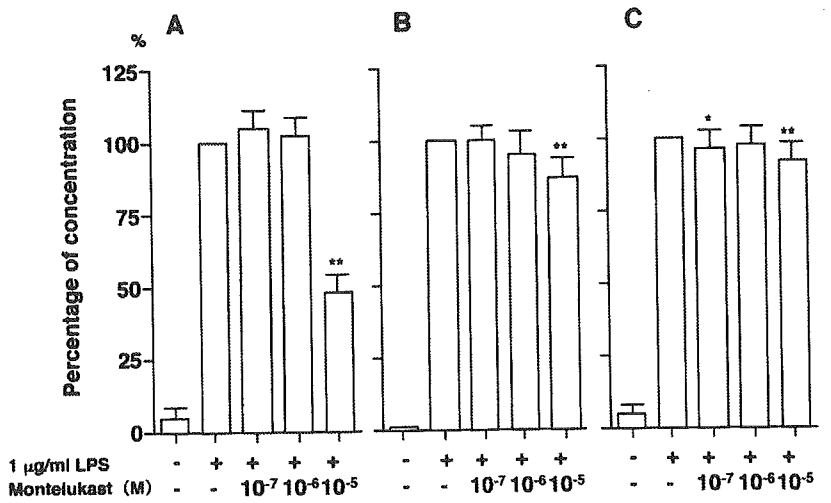

Figure 4. Inhibitory effect of montelukast on interleukin 6 (A), tumor necrosis factor α (B), and monocyte chemoattractant protein 1 (C) releases, as measured by enzyme-linked immunosorbent assay, in the peripheral blood mononuclear cells (PBMCs) of controls stimulated with lipopolysaccharide (LPS) for 2 hours, with pretreatment with montelukast for 30 minutes. Data (n = 8) were expressed taking the value for cytokine concentrations in culture fluids of PBMCs treated with LPS only as 100% and are presented as mean +1 SD. Double asterisk indicates $P < .01$; asterisk, $P < .05$ compared with culture fluid of PBMCs treated with LPS only.

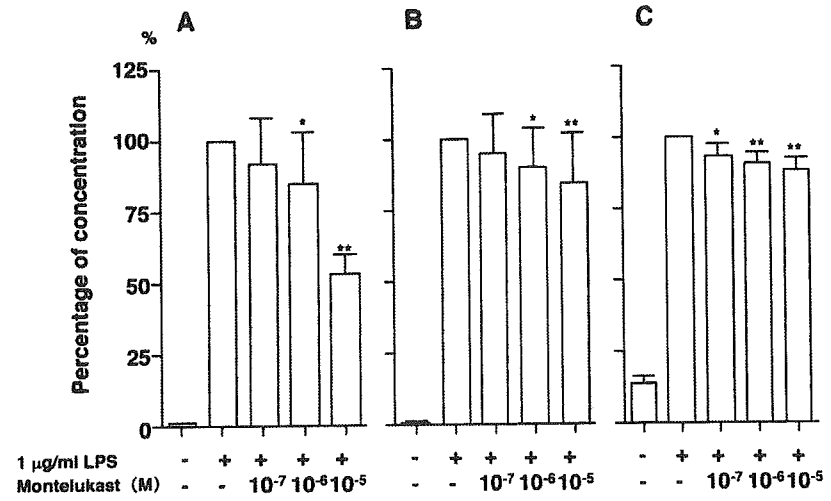

Figure 5. Inhibitory effect of montelukast on interleukin 6 (A), tumor necrosis factor α (B), and monocyte chemoattractant protein 1 (C) releases, as measured by enzyme-linked immunosorbent assay, in the peripheral blood mononuclear cells (PBMCs) of patients with asthma stimulated with lipopolysaccharide (LPS) for 2 hours, with pretreatment with montelukast for 30 minutes. Data (n = 8) were expressed taking the value for cytokine concentrations in culture fluids of PBMCs treated with LPS only as 100% and are presented as mean +1 SD. Double asterisk indicates $P < .01$; asterisk, $P < .05$ compared with culture fluid of PBMCs treated with LPS only.

macrophages are activated by bacterial products and viruses and produce proinflammatory molecules. In addition, the role of monocytes and macrophages in allergic inflammation has been focused on. Activation of monocytes and macrophages results in the promotion of inflammation. Proinflammatory molecules produced by monocytes and macrophages are reported to have a variety of effects. Interleukin 6 produces local inflammatory reactions by amplifying leukocyte recruitment and inducing antibody production.[21] Tumor necrosis factor α causes interstitial pulmonary edema by altering the lung endothelial barrier.[22] Furthermore, TNF-α binding to the type 1 TNF receptor induces NF-κB activation and releases more proinflammatory molecules.[23] Monocyte chemoattractant protein 1 recruits mast cells, monocytes, $CD4^+/CD8^+$ lymphocytes, and eosinophils.[24,25] It is a histamine- and leukotriene-releasing agent for basophils and mast cells, and it enhances T_H2 polarization.[26] The proinflammatory molecules produced by monocytes and macrophages in

infectious inflammation may mediate allergic inflammation in asthma.

In adults administered a single oral dose of 102 mg, the mean ± SD maximum drug concentration was 3.61 ± 0.86 μg/mL (5.94 ± 1.41 × 10^{-6}M),[27] but this value included the contribution of montelukast bound to plasma protein. Therefore, the contribution of this effect to the anti-inflammatory activity of montelukast at therapeutic doses in patients with asthma remains unclear. In summary, high doses of montelukast modulate the production of IL-6, TNF-α, and MCP-1 through the inhibition of NF-κB activation. However, the anti-inflammatory effect of montelukast at therapeutic doses in patients with asthma needs to be further investigated.

REFERENCES

1. Lynch KR, O'Neill GP, Liu Q, et al. Characterization of the human cysteinyl leukotriene CysLT1 receptor. *Nature*. 1999; 399:789–793.
2. Figueroa DJ, Breyer RM, Defoe SK, et al. Expression of the cysteinyl leukotriene 1 receptor in normal human lung and peripheral blood leukocytes. *Am J Respir Crit Care Med*. 2001; 163:226–233.
3. Wu AY, Chik SC, Chan AW, et al. Anti-inflammatory effects of high-dose montelukast in an animal model of acute asthma. *Clin Exp Allergy*. 2003;33:359–366.
4. Frieri M, Therattil J, Wang SF, Huang CY, Wang YC. Montelukast inhibits interleukin-5 mRNA expression and cysteinyl leukotriene production in ragweed and mite-stimulated peripheral blood mononuclear cells from patients with asthma. *Allergy Asthma Proc*. 2003;24:359–366.
5. Collart MA, Baeuerle P, Vassalli P. Regulation of tumor necrosis factor alpha transcription in macrophages: involvement of four κB-like motifs and of constitutive and inducible forms of NF-κB. *Mol Cell Biol*. 1990;10:1498–1506.
6. Libermann TA, Baltimore D. Activation of interleukin-6 gene expression through the NF-κB transcription factor. *Mol Cell Biol*. 1990;10:2327–2334.
7. Hiscott J, Marois J, Garoufalis J, et al. Characterization of a functional NF-κB site in the human interleukin 1β promoter: evidence for a positive autoregulatory loop. *Mol Cell Biol*. 1993;13:6231–6240.
8. Matsusaka T, Fujikawa K, Nishio Y, et al. Transcription factors NF-IL6 and NF-κB synergistically activate transcription of the inflammatory cytokines, interleukin 6 and interleukin 8. *Proc Natl Acad Sci U S A*. 1993;90:10193–10197.
9. Kunsch C, Lang RK, Rosen CA, Shannon MF. Synergistic transcriptional activation of the IL-8 gene by NF-κB p65 (RelA) and NF-IL-6. *J Immunol*. 1994;153:153–164.
10. Baeuerle PA, Henkel T. Function and activation of NF-κB in the immune system. *Annu Rev Immunol*. 1994;12:141–179.
11. Baldwin AS Jr. The NF-κB and IκB proteins: new discoveries and insights. *Annu Rev Immunol*. 1996;14:649–683.
12. Brown K, Gerstberger S, Carlson L, et al. Control of IκB-α proteolysis by site-specific, signal-induced phosphorylation. *Science*. 1995;267:1485–1488.
13. Kumar A, Haque J, Lacoste J, et al. Double-stranded RNA-dependent protein kinase activates transcription factor NF-κB by phosphorylating IκB. *Proc Natl Acad Sci U S A*. 1994;91: 6288–6292.
14. Pyatt DW, Stillman WS, Yang Y, et al. An essential role for NF-κB in human CD34(+) bone marrow cell survival. *Blood*. 1999;93:3302–3308.
15. Ichiyama T, Nishikawa M, Yoshitomi T, et al. Clarithromycin inhibits NF-κB activation in human peripheral blood mononuclear cells and pulmonary epithelial cells. *Antimicrob Agents Chemother*. 2001;45:44–47.
16. Ichiyama T, Hasegawa S, Umeda M, et al. Pranlukast inhibits NF-κB activation in human monocytes/macrophages and T cells. *Clin Exp Allergy*. 2003;33:802–807.
17. Jones TR, Labelle M, Belley M, et al. Pharmacology of montelukast sodium (Singulair), a potent and selective leukotriene D4 receptor antagonist. *Can J Physiol Pharmacol*. 1995;73: 191–201.
18. Leyko BT, Perlman B, Huang Y, Frieri M. Assessment of RANTES mRNA production and expression in respiratory syncytial virus (RSV) antigen–stimulated and IL-1β–stimulated A549 cells: inhibition via montelukast and budesonide [abstract]. *Ann Allergy Asthma Immunol*. 2004;92:115.
19. Ng DK, Law AK, Chau KW, Chan HK. Use of montelukast in the treatment of early childhood wheezing from clinical experience with three cases. *Respirology*. 2000;5:389–392.
20. Holgate ST, Peters-Golden M, Panettieri RA, Henderson WR Jr. Roles of cysteinyl leukotrienes in airway inflammation, smooth muscle function, and remodeling. *J Allergy Clin Immunol*. 2003;111:S18–S34.
21. Romano M, Sironi M, Toniatti C, et al. Role of IL-6 and its soluble receptor in induction of chemokines and leukocyte recruitment. *Immunity*. 1997;6:315–325.
22. Chen R, Gao B, Huang C, et al. Transglutaminase-mediated fibronectin multimerization in lung endothelial matrix in response to TNF-α. *Am J Physiol Lung Cell Mol Physiol*. 2000; 279:161–171.
23. Christman JW, Lancaster LH, Blackwell TS. Nuclear factor κB: a pivotal role in the systemic inflammatory response syndrome and new target for therapy. *Intensive Care Med*. 1998;24: 1131–1138.
24. Campbell EM, Charo IF, Kunkel SL, et al. Monocyte chemoattractant protein-1 mediates cockroach allergen-induced bronchial hyperreactivity in normal but not $CCR2^{-/-}$ mice: the role of mast cells. *J Immunol*. 1999;163:2160–2167.
25. Dunzendorfer S, Kaneider NC, Kaser A, et al. Functional expression of chemokine receptor 2 by normal human eosinophils. *J Allergy Clin Immunol*. 2001;108:581–587.
26. Rose CE Jr, Sung SS, Fu SM. Significant involvement of CCL2 (MCP-1) in inflammatory disorders of the lung. *Microcirculation*. 2003;10:273–288.
27. Balani SK, Xu X, Pratha V, et al. Metabolic profiles of montelukast sodium (Singulair), a potent cysteinyl leukotriene 1 receptor antagonist, in human plasma and bile. *Drug Metab Dispos*. 1997;25:1282–1287.

Requests for reprints should be addressed to:
Takashi Ichiyama, MD
Department of Pediatrics
Yamaguchi University School of Medicine
1-1-1 Minamikogushi
Ube, Yamaguchi 755-8505, Japan
E-mail: ichiyama@yamaguchi-u.ac.jp

Paraneoplastic cerebellar degeneration in olfactory neuroepithelioma

Anti-Hu antibody was first discovered in patients with paraneoplastic encephalomyelitis associated with small cell lung cancer (SCLC). This antibody recognises proteins comprised in the Hu family expressed by neuronal cells as well as SCLC. After the first report, anti-Hu antibody was found in other neoplasms including prostate and breast cancer, adrenal carcinoma, chondromyxosarcoma, neuroblastoma, and neuroendocrine neoplasms at other sites.[1] Olfactory neuroepithelioma (9523/3)[2] is thought to differ from classic neuroblastoma (9500/3) in its expression pattern of tyrosine hydroxylase, *MYCN* amplification, and fusion of the Ewing sarcoma gene and the Friend leukaemia virus integration 1 gene or the ETS related gene.[3]

Anti-Hu antibody in association with olfactory neuroepithelioma has not been reported previously. We report a patient with cerebellar ataxia that paralleled the recurrence of the tumour. Serum and cerebrospinal fluid (CSF) from the patient contained anti-Hu antibody, and the olfactory neuroepithelioma resected from the patient expressed Hu antigen.

CASE REPORT

Seven years before admission, a 65 year old man presented with olfactory neuroepithelioma that had invaded the orbit and frontal lobe. The tumour was dissected surgically, and dura mater graft was not used in the surgery. The patient underwent irradiation (total dose of 50 Gy). The tumour recurred at the parotid gland in January 2001, and there was gait instability. The patient consulted a neurologist, but there was no specific finding. The recurrent tumour was surgically dissected; however, the instability progressed rapidly, and at the patient's admission in November 2001, he needed support when walking. There was neither alcoholism nor family history of cerebellar ataxia. His parents were not consanguineous.

General physical examination was negative. There was no lymphoadenopathy. He was alert and mentally normal. Olfactory sensation had been decreased since the first surgery, there was a downbeat nystagmus, and muscle strength was maximum. Both superficial and deep sensation were normal. Deep tendon reflex was symmetrical and normal, Romberg test was negative, and no pathological reflex was found. Nose–finger–nose test was normal, but heel–shin test was poor. Dysmetria was marked in both legs. His gait was wide based and ataxic, and tandem gait was impossible. There was no dysarthria.

Haematological studies, blood chemical analyses, and serological studies were normal. Tumour markers including α-fetoprotein, prostate specific antigen, pro-gastrin releasing peptide, neurone specific enolase, sialyl Lewis (a) (CA19–9), and sialyl Lewis (x) (SLX) were within normal limits. Levels of vitamin B1 and B12 were normal. Protein level in cerebrospinal fluid (CSF) was increased to 105 mg/dl with normal cellularity. Myelin basic protein and oligoclonal IgG band was negative. IgG index was 0.6. No malignant cells were found in the CSF. Nerve conduction study was normal. Short sensory evoked potentials of upper and lower limbs were normal. Electroencephalogram showed beta rhythm at the bilateral frontal region, with otherwise normal findings.

Computed tomography (CT) showed no lung tumour. Magnetic resonance imaging (MRI) showed bilateral leukoaraiosis at bilateral frontal lobes that had been present since after the first surgery. The cerebellum was slightly atrophic.

Titres of anti-Hu antibody in the serum and CSF were 1:1920 and 1:64, respectively (indirect immunofluorescence and Western blotting for recombinant HuD). Serum:CSF antibody titre ratio was 30. The ratio for (CSF/serum antibody titre)/(CSF/serum albumin) was 1.8. These values indicated that intrathecal synthesis of anti-Hu antibody had stopped at this time point. Other antineuronal antibodies including anti-Yo, Ri, CV2, Tr, Ma, amphiphysin, and glutamic acid decarboxylase were all negative. Systemic examination including ^{67}Ga-citrate scintigraphy did not disclose malignant tumours. Immunohistochemistry with anti-HuD antibody (Santa Cruz, sc-5977, ×100) revealed that a part of the tumour expressed Hu protein (fig 1).

Over the course of 4 years after discharge, the cerebellar ataxia did not worsen further in the absence of immunological treatment. Follow up thoracic CT and tumour marker study did not disclose other malignant tumours. There was no evidence of the recurrence of olfactory neuroepithelioma.

CONCLUSION

This patient presented cerebellar ataxia of the trunk and lower limbs that progressed rapidly within approximately 6 months after the second surgery and stabilised thereafter. This clinical course is not inconsistent with the natural course of paraneoplastic cerebellar degeneration. Although isolated cerebellar ataxia in anti-Hu antibody positive patients is rare (4/200 patients),[1] a high titre of serum anti-Hu antibody (1:1920) corroborated the diagnosis of paraneoplastic syndrome.[1] The expression of the HuD protein by the olfactory neuroepithelioma confirmed the diagnosis.

Olfactory neuroepithelioma is a neuroectodermal neoplasm that arises from the olfactory epithelium. It is distinguished from classic neuroblastoma as described by Sorensen *et al*.[3] Unlike neuroblastoma, olfactory neuroepithelioma shows differentiation to the neural processes and glandular structure and is rarely associated with catecholamine secretion. In addition, olfactory neuroepithelioma expresses epithelial markers such as cytokeratin and a 34 kDa epithelial membrane glycoprotein recognised by monoclonal antibody named Ber-EP4. The tumour in this case expressed both Ber-EP4 and cytokeratin (see Okabe *et al*[4], case no. 6). Moreover, it also expressed luteinising hormone releasing hormone. The expression pattern of Ber-EP4 and cytokeratin was heterogeneous in this tumour.[4] These findings suggest that the tumour in this case had arisen from the olfactory placode and was distinct from classic neuroblastoma arising from the neural crest.[5] This neuroepithelial tumour has not been reported to be associated with paraneoplastic syndrome. Our data clearly demonstrate the expression of Hu antigen by the olfactory neuroepithelioma cells and the presence of Hu antibody in his serum and CSF. It is interesting that neurological manifestations developed in parallel with the recurrence of the tumour. The recurrence might have enhanced immune response. Despite resection of the recurrent tumour, the cerebellar ataxia worsened for several months after surgery. However, it did not progress thereafter. In patients with neurological symptoms and Hu antibody, olfactory neuroepithelioma should be considered when a neoplasm is not found at the common sites such as the lung or breast.

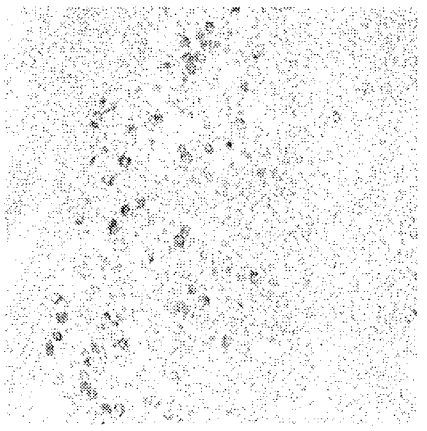

Figure 1 Immunohistochemistry using anti-HuD antibody. A part of the patient's tumour expressed HuD antigen (×400).

K Maeda, T Sasaki, Y Murata, M Kanasaki, T Terashima, H Kawai, H Yasuda
Division of Neurology, Department of Medicine, Shiga University of Medical Science, Otsu, Shiga, Japan 520-2192

H Okabe
Department of Clinical Laboratory Medicine, Shiga University of Medical Science, Otsu, Shiga, Japan 520-2192

K Tanaka
Department of Neurology, Brain Research Institute, Niigata University, Niigata, Japan

Correspondence to: Kengo Maeda, Division of Neurology, Department of Medicine, Shiga University of Medical Science, Otsu, Shiga, Japan 520-2192; kengo@belle.shiga-med.ac.jp

doi: 10.1136/jnnp.2005.066977

Received 6 March 2005

In revised form 20 April 2005

Accepted 22 May 2005

Competing interests: there are no competing interests

REFERENCES

1 **Graus F**, Keime-Guibert F, Reñe R, *et al*. Anti-Hu-associated paraneoplastic encephalomyelitis: analysis of 200 patients. *Brain* 2001;**124**:1138–48.
2 In: **Kleihues P**, Cavenee WK, eds. *World Health Organisation classification of tumours: pathology and genetics of tumours of the nervous system*. Lyon: IARC Press, 2000.
3 **Sorensen PHB**, Wu JK, Berean KW, *et al*. Olfactory neuroblastoma is a peripheral primitive neuroectodermal tumor related to Ewing sarcoma. *Proc Natl Acad Sci USA* 1996;**93**:1038–43.
4 **Okabe H**, Okubo T, Ochi Y. On the origin and diagnostic criteria of olfactory neuroblastoma. *Acta Histochem Cytochem* 1997;**30**:181–8.
5 **Okabe H**, Okubo T, Ochi Y. Expression of epithelial membrane glycoprotein by neurons arising from olfactory plate through development. *Neuroscience* 1996;**72**:579–84.

ABSTRACT: Previous studies suggest that the muscle fiber lysosome system plays a central role in the increased formation of autophagosomes and autolysosomes that occurs in the context of chloroquine-induced myopathy. The goal of this study was to characterize the contribution of receptor-mediated intracellular transport, particularly the endosomal pathway, to the abnormal accumulation of vacuoles in experimental chloroquine myopathy. Expression of the mannose 6-phosphate receptor (M6PR) and clathrin were analyzed in innervated and denervated rat soleus muscles after treatment with either saline or chloroquine. Accumulation of vacuoles was observed only in chloroquine-treated denervated muscles. Further, clathrin immunostaining and M6PR messenger ribonucleic acid (mRNA) were significantly increased in denervated soleus muscle from saline- and chloroquine-treated rats compared to contralateral, innervated muscles. However, there was no difference in clathrin levels when comparing saline- and chloroquine-treated denervated muscles. These data suggest that chloroquine activates the transport of newly synthesized lysosomal enzymes from the secretory pathway via the trans-Golgi network of the Golgi apparatus (an endosomal pathway) as well as autophagosome formation (an autophagic process) in skeletal muscles. Vacuoles may subsequently accumulate secondary to abnormal formation or turnover of autolysosomes at or after fusion of autophagosomes with early endosomes.

Muscle Nerve **31:** 495–502, 2005

SKELETAL MUSCLE EXPRESSION OF CLATHRIN AND MANNOSE 6-PHOSPHATE RECEPTOR IN EXPERIMENTAL CHLOROQUINE-INDUCED MYOPATHY

TOMOKO MASUDA, MD,[1] HIDETSUGU UEYAMA, MD,[1] KEN-ICHIRO NAKAMURA, MD,[1] MIKA JIKUMARU, MD,[1] ITARU TOYOSHIMA, MD,[2] and TOSHIHIDE KUMAMOTO, MD[1]

[1] Department of Neurology and Neuromuscular Disorders, Oita University Faculty of Medicine, Idaigaoka 1-1, Hasama, Oita 879-5593, Japan
[2] First Department of Internal Medicine, Akita University School of Medicine, Akita, Japan

Accepted 6 December 2004

Chloroquine, a lysosomotrophic agent, modulates autophagic protein degradation in the lysosome system, thereby inducing the formation of rimmed vacuoles (e.g., autophagosomes/autolysosomes) in skeletal muscle.[11,14,25] Chloroquine, in vitro, accumulates within lysosomes and causes a pronounced elevation of interlysosomal pH, and thus indirectly blocks the lysosomal acidic proteases, specifically cathepsin B.[21] Subsequently, material normally degraded by lysosomes will accumulate in proportion to the inhibitory effect on the enzymes responsible for their degradation, and numerous rimmed vacuoles will form in the muscles. However, previous studies have demonstrated that the activity of lysosomal proteases, including cathepsins B and L, is increased in the skeletal muscles of chloroquine-treated rats. At any rate, no decrease in cathepsin B activity was shown in the chloroquine-treated muscles in vivo, contrary to previous reports.[11]

We previously demonstrated an increased number of dense granular bodies and vacuoles in denervated chloroquine-treated rat muscle and the absence of these findings in contralateral, innervated chloroquine-treated muscle and in the innervated and denervated muscles of saline-treated rats.[14] In general, denervation stimulates endocytosis and the breakdown of muscle fibers, with many phagosomes and autophagosomes being formed in the skeletal muscles.[1,17] Usually, these vacuoles are too small to

Abbreviations: cDNA, complementary DNA; DNA, deoxyribonucleic acid; M6PR, mannose 6-phosphate receptor; mRNA, messenger RNA; PCR, polymerase chain reaction; RNA, ribonucleic acid; rRNA, ribosomal RNA; SDS, sodium dodecyl sulfate; SSPE, sodium chloride, sodium dihydrogen phosphate, di-sodium hydrogen phosphate, and ethylenediaminetetraacetic acid (EDTA); TGN, trans-Golgi network

Key words: chloroquine; clathrin; lysosome; mannose 6-phosphate receptor; mRNA; muscle; Northern blot

Correspondence to: T. Kumamoto; e-mail: kumagoro@med.oita-u.ac.jp

Published online 14 February 2005 in Wiley InterScience (www.interscience.wiley.com). DOI 10.1002/mus.20288

be observable by light microscopy. Chloroquine-only treatment for about 1 month induces numerous autophagosomes in rat skeletal muscles that are visible under the light microscope, whereas vacuoles are rare in muscles from rats given chloroquine for 2–3 weeks.[11] Our previous study showed, however, that denervation produced a remarkable accumulation of autophagosome within 2 weeks after chloroquine-only treatment of muscles, when hardly any such vacuoles would otherwise be seen under light microscopy. Further, the activity of the lysosomal enzymes, cathepsins B and L, was significantly increased in the denervated muscles from saline- and chloroquine-treated rats relative to the contralateral, innervated muscles.[12,14] Interestingly, while vacuoles were only increased in chloroquine-treated denervated muscles, there was no difference in lysosomal enzyme activity when comparing saline-treated and chloroquine-treated denervated muscles. Since an autophagic-lysosome process as well as nonlysosomal process (i.e., calpain and ubiquitin-proteasome proteolytic pathways[19,26]) mediate degradation of muscle fibers in denervated muscles,[14] chloroquine-induced dysfunction of the autophagic-lysosome process could represent an excellent mechanistic explanation for vacuole formation.

The autophagic-lysosome system plays an important role in the degradation and turnover of intracellular proteins and organelles in skeletal muscle.[1,5,6] This system consists of an autophagic process, an endosomal pathway, and an autolysosomal degradation process. Denervation causes marked muscle breakdown, after which numerous autophagosomes are formed (an autophagic process). At the same time, generation of early endosomes is increased and reflected by the formation of lysosomal enzyme-containing clathrin-coated vesicles from the trans-Golgi network (TGN) of the Golgi apparatus (an endosomal pathway). The fusion of autophagosome with early endosomes subsequently leads to formation of autolysosomes, in which the segregated cellular components in the autophagosome are degraded by lysosomal enzymes such as cathepsins and other acid hydrolases from early endosome (an autolysosomal degradation process).[1,5] Although these pathways have been well characterized, it is not clear how chloroquine treatment affects the autophasic-lysosome system.

In general, activation of autophagy mediates the transport of newly synthesized lysosomal enzymes from the exocytotic pathway via the TGN to the early endosome.[16] Receptor-mediated intracellular transport pathways and formation of early endosomes and autolysosomes involve many signal transduction elements, including mannose-6-phosphate receptor (M6PR), clathrin, adaptins, and coatomer proteins.[9,15,24] Specifically, M6PR recycles between the TGN and the early endosomes for transport of newly synthesized lysosomal enzymes,[2] and clathrin coats the vesicles involved in the export of aggregated materials from the TGN and the transfer of lysosomal enzymes from the TGN to the lysosomes.[3,22,23]

The goal of this study was to characterize the contribution of receptor-mediated intracellular transport, particularly the endosomal pathway, to the abnormal accumulation of vacuoles in experimental chloroquine myopathy through the use of histologic, immunohistochemical, and Northern blot studies of innervated and denervated rat muscles.

MATERIALS AND METHODS

Animals. The left hind-legs of 40 adult male Wistar rats (200–250 g) were denervated by ligation of the sciatic nerve, as previously described.[14] Chloroquine chloride (50 mg/kg body weight) was injected intraperitoneally into 20 rats twice daily, beginning on the day after denervation. The remaining 20 rats received injection of saline. The soleus muscles from the right (innervated) and left (denervated) legs were obtained from the chloroquine- and saline-treated rats on days 1, 2, 4, and 8 after the initial injection. The muscles were then rapidly frozen in isopentane cooled in liquid nitrogen.

Histological and Immunohistochemical Studies. Routine histological analysis was performed using cryostat sections (10-μm thick), as described previously.[14,20] Hematoxylin–eosin preparations of each specimen were analyzed with a Nikon Cosmozon ISA image analyzer (Nikon, Tokyo, Japan) attached to a Macintosh computer (Apple Computer, Cupertino, California). The number of fibers with dense granular bodies or vacuoles at the light microscopic level was determined in 400 muscle fibers per muscle.

For immunohistochemical analysis, sections were incubated for 1 h at room temperature in 1:30 diluted mouse monoclonal anti-clathrin antibody (Progen Biotechnik GmbH, Heidelberg, Germany). After incubation with alkaline phosphatase–conjugated goat anti-mouse immunoglobulin (Ig) M (Vector Lab., Burlingame, California) for 30 min, the sites of antibody binding were visualized by staining with the Alkaline Phosphatase Substrate Kit I (Vector Red; Vector Lab.) for 30 min. The sections were then counterstained with hematoxylin.

Isolation of RNA. Innervated and denervated soleus muscles from saline- and chloroquine-treated rats were excised and frozen rapidly in liquid nitrogen. Total ribonucleic acid (RNA) was isolated from specimens using acid guanidinium thiocyanate buffer (Nippon Gene, Tokyo, Japan), according to the manufacturer's instructions. Purity and integrity of the RNA was assured by using 1% agarose gel electrophoresis under denaturing conditions.

Preparation of Rat cDNA Probe. Polymerase chain reaction (PCR) primers were constructed on the basis of published nucleotide sequences of the mouse M6PR gene[18] (Nos. 83-100, 5′-GCT GCT GGA CTG AAC-3′, sense; Nos. 624–641, 5′-ATC GAG CCC ACA CTG AGG-3′, antisense) and the rat clathrin heavy chain gene[8] (5′-GTG TTC CTG ATT ACC AAG-3′, sense; 5′-CCA CAG ATT TTA CGA GAR-3′, antisense). Complementary deoxyribonucleic acid (cDNA) was synthesized from 1 μg of total RNA using 200 units of Moloney murine leukemia virus reverse transcriptase (Gibco BRL, Rockville, Maryland) and 1 μg of oligo- (dT) 12–18 primer (Invitrogen, Tokyo, Japan). The PCR reactions were performed in a final volume of 50 μl in a DNA thermal cycler (ASTEC Co., Tokyo, Japan). Each PCR reaction mixture contained 1 μl of cDNA, 10 × PCR buffer (200 mM Tris-HCl, pH 8.4, and 500 mM KCl), 2.5 mM dNTP, 25 mM $MgCl_2$, 0.5 μM of each set of primers, and 2.5 units of Taq DNA polymerase (Gibco BRL). The PCR mixture was incubated at 94°C for 2 min, and 30 or 35 cycles of amplification were performed. Each cycle consisted of 1 min of denaturation at 94°C, 1 min of annealing at 50° or 55°C, and 2 min of extension at 72°C. After 30 or 35 cycles, a final extension step was performed for 5 min at 72°C. Each PCR fragment was labeled with [α-^{32}P] dcTP using the Megaprime DNA labeling system (Amersham Bioscience, Piscataway, New Jersey) before use of the PCR fragment as a probe.

Northern Blot Analysis. Total RNA (10μg) was separated on a 1% agarose gel containing 2.2 M formaldehyde before transferring to nitrocellulose membrane (Hybond N^+; Amersham, Braunschweig, Germany) in 20 × SSC by capillary blotting and cross-linking to the membrane by exposure to ultraviolet light for 2 min. ^{32}P-labeled cDNA probes of rat M6PR and clathrin were denatured at 98°C for 5 min before dilution to 37 MBq/ml in hybridization buffer of 50% formamide, 5 × SSC, 0.1% (w/v) laurylsarcosinate, and 0.02% (w/v) blocking reagent (Boehringer Ingelheim GmbH, Ingelheim, Germany). Hybridization was performed overnight at 42°C. Membranes were washed for 1 h at 60°C with 2 × SSPE of 3 M NaCl, 12 mM NaH_2PO_4, 188 mM NaH_2PO_4, and 20 mM ethylenediaminetetraacetic acid containing 0.1% sodium dodecyl sulfate–polyacrylamide (SDS) followed by 0.1 × SSPE containing 0.1% SDS for 1 h at 60°C. Quantification of signals was performed using a Bio-image analyzer BAS 2000II (Fuji Film, Tokyo, Japan) radioisotope detector (Raytest, Straubenhardt, Germany). Ethidium bromide staining of ribosomal RNA (rRNA) was used to quantify the amounts of RNA species on the blots.

Statistical Analysis. Differences between control specimens and disease specimens were evaluated with the unpaired *t*-test. A *P*-value of <0.05 was considered statistically significant.

RESULTS

Histological and Immunohistochemical Studies. Histological findings for the innervated and denervated soleus muscles from saline- and chloroquine-treated rats on each test day were consistent with previous reports[14,20] (Fig. 1). Dense granular bodies and vacuoles were more numerous in chloroquine-treated muscles after denervation, particularly on day 8. In contrast, there were relatively few dense granular bodies and vacuoles in the contralateral, innervated chloroquine-treated muscles. Quantitative analysis at the light microscopic level showed that the number of fibers with dense granular bodies or vacuoles in innervated and denervated muscles from rats after chloroquine treatment, respectively, was 1.5 ± 0.6% and 1.8 ± 1.0% on day 1, 9.4 ± 3.8% and 12.7 ± 7.8% on day 2, 6.7 ± 1.7% and 19.5 ± 5.0% on day 4 ($P = 0.0006$), and 2.7 ± 1.5% and 51.9 ± 14.6% on day 8 ($P < 0.0001$). Vacuoles were present in only a few fibers in innervated and denervated muscles from saline-treated rats.

Clathrin staining was minimal in innervated muscles from saline- and chloroquine-treated rats at all time points, whereas denervated muscles from both groups showed progressively stronger clathrin staining with increasing time (Fig. 2). Strong positive reactions for clathrin were often observed inside and in the area surrounding vacuoles in the denervated muscles of chloroquine-treated rats, although these muscles did not show more advanced changes than the denervated muscles of saline-treated rats. The denervated muscles of chloroquine-treated rats showed more advanced changes than saline-treated rats. Increased clathrin-positive granules were observed in the sarcoplasm, especially in the muscle

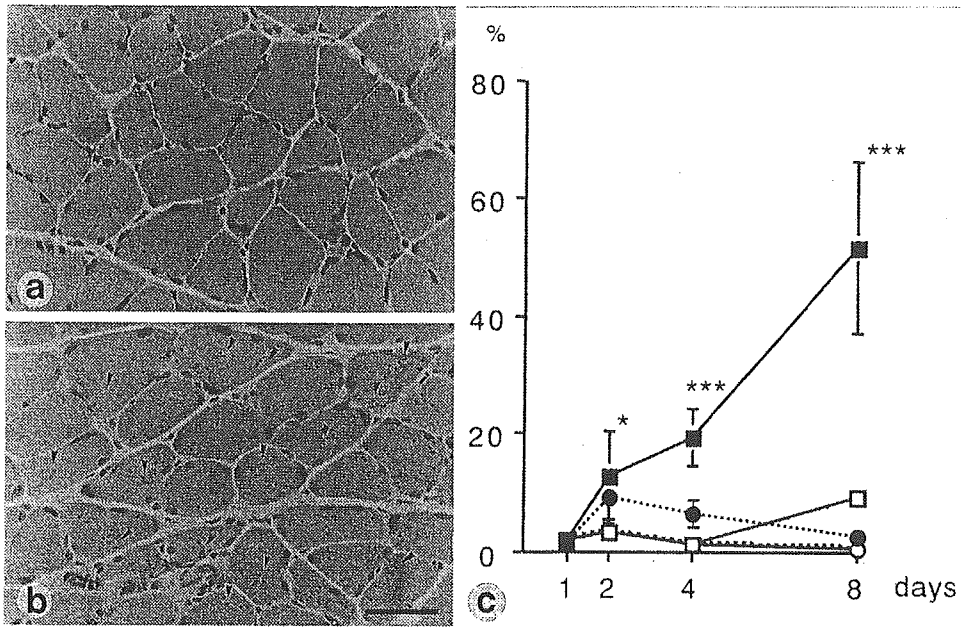

FIGURE 1. (a,b) Cross sections of rat soleus muscles after 8 days of saline or chloroquine treatment. The left denervated muscle from rats treated with saline **(a)** and chloroquine **(b)** shows moderate muscle fiber atrophy. A large number of dense granular bodies and vacuoles (arrowheads) are present in the denervated muscle from chloroquine-treated rats **(b)** but are absent in denervated muscles from saline-treated rats (a). Stained with hematoxylin-eosin (H&E). Bar, 50 μm. **(c)** Incidence of fibers with dense granular bodies and vacuoles in muscle fibers from rats after chloroquine or saline treatment. Points represent means ± standard deviations (vertical lines). Number of rats per group = 5. ○, innervated muscle from saline-treated rats; ●, innervated muscles from chloroquine-treated rats; □, denervated muscle from saline-treated rats; ■, denervated muscle from chloroquine-treated rats. $^{*}P < 0.05$; $^{***}P < 0.0001$ versus the value for innervated muscle from saline-treated rats.

fibers containing vacuoles, and occasionally in the vacuoles themselves.

M6PR and Clathrin mRNA Levels. Clathrin and M6PR messenger RNA (mRNA) levels were measured in the innervated and denervated soleus muscles of saline- and chloroquine-treated rats at various times (Figs. 3 and 4). Elevations in M6PR mRNA occurred as early as day 2 in the denervated muscles from chloroquine-treated rats (1.2-, 1.9-, 2.1-, and 1.7-fold increases relative to innervated muscles from saline-treated rats on days 1, 2, 4, and 8, respectively), but reached the level of statistical significance only on days 2 and 4. In the denervated muscles from saline-treated rats, M6PR mRNA increased to 1.1-, 1.3-, 1.4-, and 1.5-fold those of innervated muscles from saline-treated rats on days 1, 2, 4, and 8, respectively (on day 8, $P < 0.01$). M6PR mRNA levels appeared higher in denervated muscles from chloroquine-treated rats than from saline-treated rats, but the difference was not statistically significant (Fig. 3).

Clathrin mRNA levels in denervated muscles from saline-treated rats were 1.1-, 1.0-, 1.3-, and 1.2-fold those of innervated muscles from saline-treated rats on days 1, 2, 4, and 8, respectively. Further, clathrin mRNA levels in the denervated muscle from chloroquine-treated rats were 1.3-, 1.0-, 1.7-, and 1.3-fold those of innervated muscles from saline-treated rats on days 1, 2, 4, and 8, respectively. However, clathrin mRNA levels were similar when comparing denervated muscles of both groups on each test day. Clathrin mRNA levels peaked on day 4, whereas the increase in protein expression and vacuole formation persisted on day 8 (Fig. 4).

DISCUSSION

The present study demonstrated an increase in dense granular bodies and vacuoles (primarily autophagosomes and, to a lesser extent, autolysosomes) in the denervated soleus muscles from chloroquine-treated rats, which is consistent with previous reports.[14,20] An increase in vacuolar formation was observed as early as day 2, with progressive increases thereafter. In contrast, relatively few such structures were present in innervated and denervated muscles from saline-treated rats. This suggests that chloroquine treatment inhibits lysosomal proteolysis or turnover in denervated muscles, thereby resulting in increased formation of autophagosomes and autolysosomes.[14,20] However, since the granules are mem-

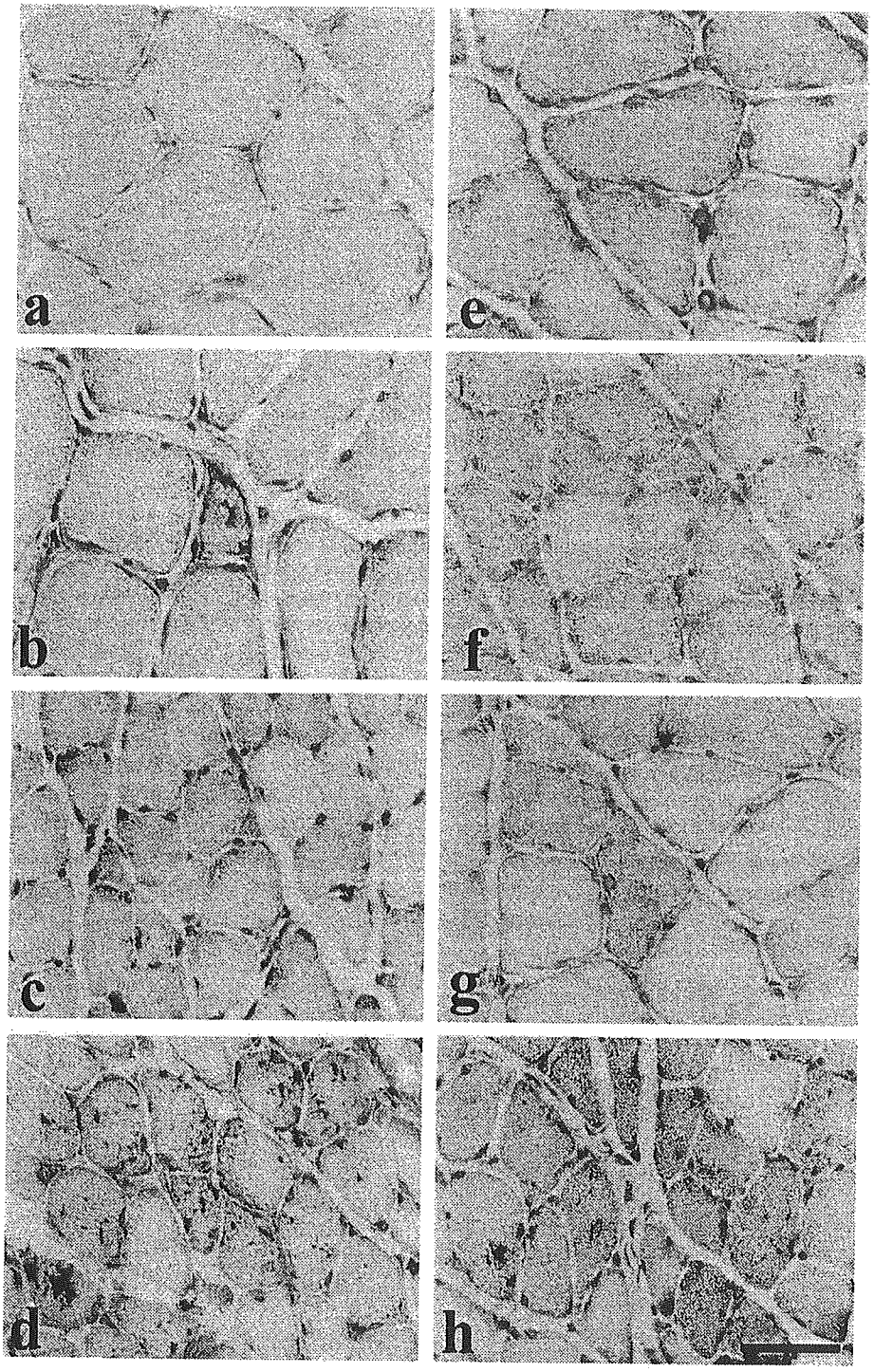

FIGURE 2. Immunostaining for anti-clathrin antibodies in innervated and denervated rat soleus muscles after saline or chloroquine treatment. Immunoreactivity for clathrin is increased in the denervated muscles from rats treated with saline **(c)** and chloroquine **(d)** compared to the innervated muscle from saline **(a)** and chloroquine-treated rats **(b).** Strong positive reactions for clathrin are seen inside and in the area surrounding vacuoles in the denervated muscles of chloroquine-treated rats **(d)** although these muscles do not show more advanced changes than the denervated muscles of saline-treated rats **(c).** In denervated rat soleus muscles on days 1, 2, 4, and 8 of chloroquine treatment, immunoreactivity for clathrin in muscle fibers shows a progressive increase with time **(e–h). (a–d)** on day 8; **(e)** on day 1; **(f)** on day 2; **(g)** on day 4; **(h)** on day 8. Bar, 50 μm.

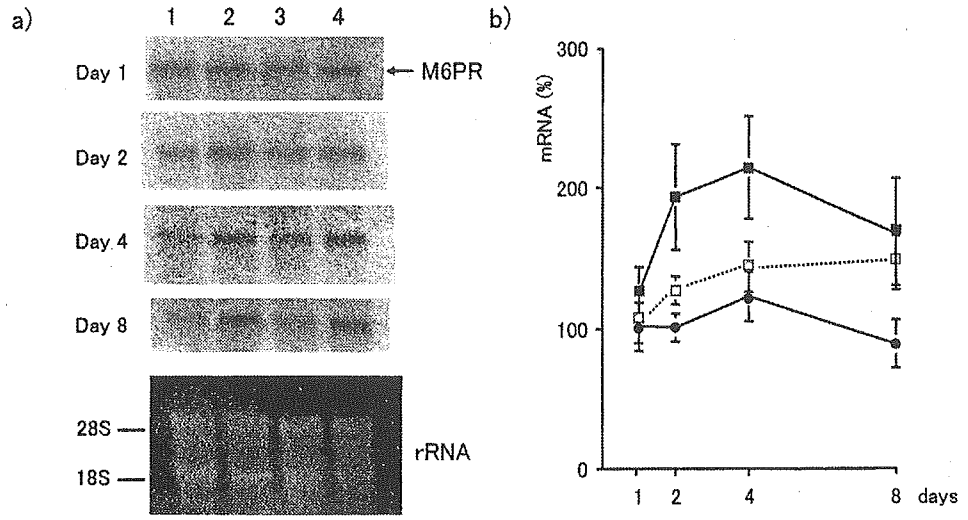

FIGURE 3. (a) Northern blot analysis of relative mannose 6-phosphate receptor (M6PR) mRNA levels in innervated and denervated soleus muscles from saline- and chloroquine-treated rats on days 1, 2, 4, and 8. **(b)** Changes in M6PR mRNA levels in innervated and denervated rat soleus muscles on days 1, 2, 4, and 8 of saline or chloroquine treatment. Values are normalized to the M6PR mRNA level in innervated muscle of saline-treated rats (control muscle). Points represent mean ± SD. Number of rats per group = 5. ●, innervated muscles from chloroquine-treated rats; □, denervated muscle from saline-treated rats; ■, denervated muscle from chloroquine-treated rats. rRNA, ribosomal RNA.

branous, inhibition of breakdown of complex lipids as well as proteins is probably just as important.

Clathrin and M6PR play a central role in the endosomal pathway. Clathrin-coated vesicles are involved in three receptor-mediated intracellular transport pathways: export of aggregated material from the TGN for regulated secretion, transfer of lysosomal enzymes from the TGN to the early endosome, and receptor-mediated endocytosis at the plasma membrane.[3,22,23] In the present study, immunohistochemical analysis found that most normal muscle fibers did not express clathrin in their sarcoplasm. Further, clathrin-positive granules were more abundant in the sarcoplasm of denervated muscles

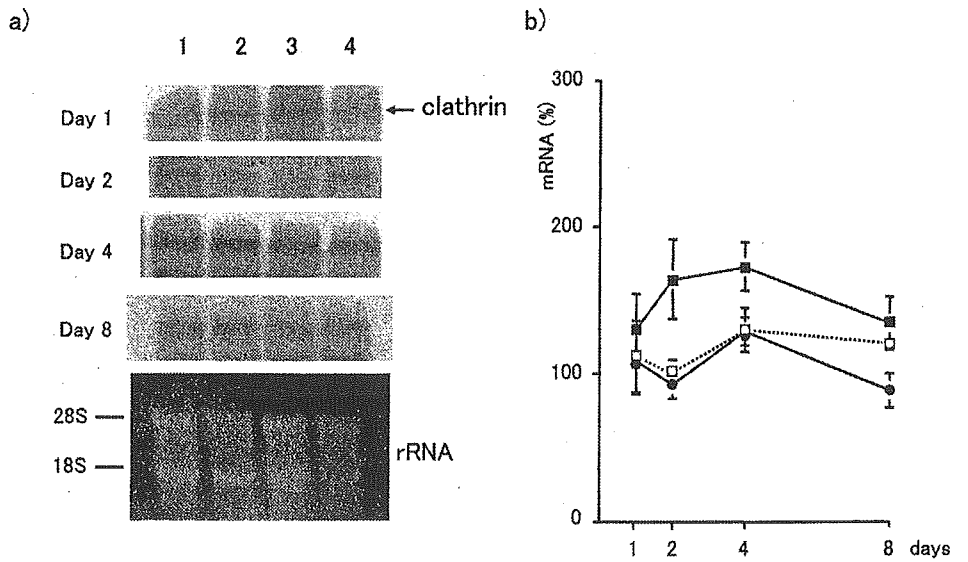

FIGURE 4. (a) Northern blot analysis of relative clathrin mRNA levels in innervated and denervated soleus muscles from saline- and chloroquine-treated rats on days 1, 2, 4, and 8. **(b)** Changes in clathrin mRNA in innervated and denervated rat soleus muscles on days 1, 2, 4, and 8 of saline or chloroquine treatment. Values are normalized to the clathrin mRNA level in innervated muscle of saline-treated rats (control muscle). Points represent mean ± SD. Number of rats per group = 5. ●, innervated muscles from chloroquine-treated rats; □, denervated muscle from saline-treated rats; ■, denervated muscle from chloroquine-treated rats. rRNA, ribosomal RNA.

from saline- and chloroquine-treated rats than their contralateral, innervated muscles. Although there was no difference in staining activity for clathrin when comparing denervated muscles from both animal groups, clathrin-positive granules were present in vacuoles in denervated, chloroquine-treated muscles. We previously reported that clathrin levels were significantly elevated in denervated soleus muscles on Western immunoblot.[12] In the present study, clathrin levels were elevated in denervated muscles from both chloroquine-treated and saline-treated rats, despite the difference in abundance of vacuoles. These results suggest that denervation may increase receptor-mediated intracellular transport (i.e., trafficking of clathrin) and that chloroquine treatment does not inhibit this transport.[13,23]

The present study demonstrated that clathrin mRNA levels were increased on day 4 in denervated muscles of saline- or chloroquine-treated rats relative to those in innervated muscles from saline-treated rats. However, these changes did not reach statistical significance. We previously demonstrated that significant increases in clathrin protein levels occurred as early as day 4 in the denervated muscles from chloroquine-treated rats and that clathrin protein increased to 7.5-fold that of the innervated, saline-treated rats on day 8.[12] The present study demonstrated a progressive increase in immunohistochemical staining for clathrin in the denervated muscles of both groups relative to that in contralateral, innervated muscles. Further, the clathrin mRNA levels in denervated muscles of chloroquine-treated rats were consistently higher than those of saline-treated rats, although the changes were small.

M6PR is expressed in the Golgi apparatus, the TGN, prelysosomal compartments, the endosome, and the plasma membrane[18] and mediates the transport of newly synthesized lysosomal enzymes from the secretory pathway to the early endosome via the TGN.[4,9,15,16,24] The present study demonstrated significantly increased levels of M6PR mRNA in the denervated muscles of saline- and chloroquine-treated rats when compared to levels in contralateral, innervated muscles. The increased M6PR in denervated muscles may result in an increase lysosomal enzyme transport from the TGN to the early endosome.

Previous report suggests that chloroquine inhibits the normal trafficking of clathrin in muscle cells.[7] However, we found that clathrin was increased in denervated muscles from saline- and chloroquine-treated rats compared with their contralateral innervated muscles, although there were no differences in clathrin expression in the denervated muscles of both groups, consistent with previous reports.[12] Further, increases in M6PR mRNA levels were observed in the denervated muscles of both groups. These results suggest that chloroquine activates the transport of newly synthesized lysosomal enzymes from the exocytotic pathway to the early endosome via the TGN, but does not inhibit. We speculate that chloroquine inhibits the autophagic-lysosome system at or after fusion of early endosomes with autophagosomes (i.e., autolysosomal degradation process). It seems that remarkable accumulation of vacuoles occurs in denervated muscles after chloroquine treatment because of abnormal lysosome function, especially the formation or turnover of autolysosome after the fusion of autophagosomes with the early endosome. Further studies are needed to confirm our hypothesis.

We are grateful to Ms. M. Ono, Ms. K. Hirano, and Ms. Y. Umeki for technical assistance.

REFERENCES

1. Bird JWC. Skeletal muscle lysosomes. In: Dingle JT, Dean RT, editors. Lysosomes in biology and pathology, Vol 4. Amsterdam: North-Holland; 1975. p 75–109.
2. Boker C, von Figura K, Hille-Rehfeld A. The carboxy-terminal peptides of 46 kDa and 300 kDa mannose 6-phosphatereceptors share partial sequence homology and contain information for sorting in the early endosomal pathway. J Cell Sci 1997;110:1023–1032.
3. Brodsky FM, Hill BL, Acton SL, Nathke I, Wong DH, Ponnambalam S, et al. Clathrin light chains: arrays of protein motifs that regulate coated-vesicle dynamics. Trends Biochem Sci 1991;16:208–213.
4. Bruder G, Wiedenmann B. Identification of a distinct 9S form of soluble clathrin in cultured cells and tissues. Exp Cell Res 1986;164:449–462.
5. de Duve G, Wattiaux R. Function of lysosomes. Annu Rev Physiol 1966;51:229–235.
6. Gerard KW, Hipkiss AR, Schneider DL. Degradation of intracellular protein in muscle. Lysosomal response to modified proteins and chloroquine. J Biol Chem 1988;263: 18886–18890.
7. Kaufman SJ, Bielser D, Foster RF. Localization of anti-clathrin antibody in the sarcomere and sensitivity of myofibril structure to chloroquine suggest a role for clathrin in myofibril assembly. Exp Cell Res 1990;191:227–238.
8. Kirchhausen T, Harrison SC, Chow EP, Mattaliano RJ, Ramachandran KL, Smart J, et al. Clathrin heavy chain: molecular cloning and complete primary structure. Proc Natl Acad Sci USA 1987;84:8805–8809.
9. Klumperman J, Kuliawat R, Griffith JM, Geuze HJ, Arvan P. Mannose 6-phosphate receptors are sorted from immature secretory granules via adaptor protein AP-1, clathrin, and syntaxin 6-positive vesicles. J Cell Biol 1998;141:359–371.
10. Kovacs J, Fellinger E, Karpati AP, Kovacs AL, Laszlo L, Rez G. Morphometric evaluation of the turnover of autophagic vacuoles after treatment with Triton X-100 and vinblastine in murine pancreatic acinar and seminal vesicle epithelial cells. Virchows Arch [B] 1987;53:183–190.
11. Kumamoto T, Araki S, Watanabe S, Ikebe N, Fukuhara N. Experimental chloroquine myopathy: morphological and biochemical studies. Eur Neurol 1989;29:202–207.

12. Kumamoto T, Nagao SI, Sugihara R, Abe T, Ueyama H, Tsuda T. Effect of chloroquine-induced myopathy on rat soleus muscle sarcoplasm and expression of clathrin. Muscle Nerve 1998;21:665–668.
13. Kumamoto T, Ueyama H, Tsumura H, Toyoshima I, Tsuda T. Expression of lysosome-related proteins and genes in the skeletal muscles of inclusion body myositis. Acta Neuropathol (Berl) 2004;107:59–65.
14. Kumamoto T, Ueyama H, Watanabe S, Murakami T, Araki S. Effect of denervation on overdevelopment of chloroquine-induced autophagic vacuoles in skeletal muscles. Muscle Nerve 1993;16:819–826.
15. Le Borgne R, Hoflack B. Mannose 6-phosphate receptors regulate the formation of clathrin-coated vesicles in the TGN. J Cell Biol 1997;137:335–345.
16. Lemansky P, Hasilik A, von Figura K, Helmy S, Fishman J, Fine RE, et al. Lysosomal enzyme precursors in coated vesicles derived from the exocytic and endocytic pathways. J Cell Biol 1987;104:1743–1748.
17. Libelius R, Tagerud S. Uptake of horseradish peroxidase in denervated skeletal muscle occurs primarily at the endplate region. J Neurol Sci 1984;66:273–281.
18. Ma ZM, Grubb JH, Sly WS. Cloning, sequencing, and functional characterization of the murine 46-kDa mannose 6-phosphate receptor. J Biol Chem 1991;266:10589–10595.
19. Medina R, Wing SS, Goldberg AL. Increase in levels of polyubiquitin and proteasome mRNA in skeletal muscle during starvation and denervation atrophy. Biochm J 1995;307:631–637.
20. Nagao SI, Kumamoto T, Masuda T, Ueyama H, Toyoshima I, Tsuda T. Tau expression in denervated rat muscles. Muscle Nerve 1999;22:61–70.
21. Ohkuma S, Takano T. Intralysosomal pH and its function with special reference to the effect of basic substances. Cell (Tokyo) 1981;13:127–136.
22. Pearse BM, Robinson MS. Clathrin, adaptors, and sorting. Annu Rev Cell Biol 1990;6:151–171.
23. Pley U, Parham P. Clathrin: its role in receptor-mediated vesicular transport and specialized functions in neurons. Crit Rev Biochem Mol Biol 1993;28:431–464.
24. Schekman R, Orci L. Coat proteins and vesicle budding. Science 1996;271:1526–1533.
25. Stauber WT, Hedge AM, Trout JJ, Schottelius BA. Inhibition of lysosomal function in red and white skeletal muscles by chloroquine. Exp Neurol 1981;71:295–306.
26. Ueyama H, Kumamoto T, Fujimoto S, Murakami T, Tsuda T. Expression of three calpain isoform genes in human skeletal muscles. J Neurol Sci 1998;155:163–169.